

Guiding Attention in End-to-End Driving Models

Diego Porres¹, Yi Xiao¹, Gabriel Villalonga¹, Alexandre Levy¹, Antonio M. López^{1,2}

Abstract

Vision-based end-to-end driving models trained by imitation learning can lead to affordable solutions for autonomous driving. However, training these well-performing models usually requires a huge amount of data, while still lacking explicit and intuitive activation maps to reveal the inner workings of these models while driving. In this paper, we study how to guide the attention of these models to improve their driving quality and obtain more intuitive activation maps by adding a loss term during training using salient semantic maps. In contrast to previous work, our method does not require these salient semantic maps to be available during testing time, as well as removing the need to modify the model’s architecture to which it is applied. We perform tests using perfect and noisy salient semantic maps with encouraging results in both, the latter of which is inspired by possible errors encountered with real data. Using CIL++ as a representative state-of-the-art model and the CARLA simulator with its standard benchmarks, we conduct experiments that show the effectiveness of our method in training better autonomous driving models, especially when data and computational resources are scarce.

1. Introduction

In intricate environments, human vision adeptly focuses on goal-relevant areas, while the rest undergo a more cursory catching, or may even be ignored. This purposeful and selective cognitive process is called the Visual Attention Mechanism (VAM) [3]. Inspired by VAM, over the past decade various attention mechanisms have been proposed to improve the performance of deep neural networks in different tasks such as image classification [5, 22, 31, 55, 56], natural language processing [2, 16, 41, 53, 61], and image captioning [8, 40, 48]. Early works [11, 28, 41, 60] proposed attention mechanisms for recurrent models, where its computation is performed sequentially along the positions of input and output. This sequential nature hinders parallelization in training samples, which can be problematic

with long sequences. Differently, the Transformer model [53] was the first to eschew recurrence and rely entirely on a self-attention mechanism to draw global dependencies between input and output.

Accordingly, the end-to-end driving model CIL++ [59], a pure vision-based state-of-the-art model, includes a transformer Encoder. However, as a data-driven end-to-end model, guiding its training to focus on regions of special interest remains an unsolved problem. Moreover, as a hybrid model concatenating a CNN and a Transformer Encoder, it is also difficult to obtain clear visual activation maps that could help understand the model’s driving actions.

Inspired by neuroscience, where it is stated that *attention is the flexible control of limited computational resources* [38], this paper proposes an intuitive and explicit attention-learning method to effectively guide vision-based end-to-end driving models to focus more on image content relevant to the drive. In turn, visual activation maps become more understandable. Our method is only applied at training time and does not involve modifying the underlying deep architecture of the driving model. By training CIL++ with this *attention guidance learning* method and using the CARLA simulator [18], we provide rich ablative results to show that the proposed method improves driving performance, especially under low data regimes.

Section 2 summarizes the most related literature. Section 3 draws the Attention Guidance Learning method we propose, and Section 4 shows its effectiveness experimentally. Finally, Section 5 summarizes the main conclusions and points toward future work.

2. Related Work

2.1. Imitation Learning

As a promising approach to training end-to-end systems, Imitation Learning (IL) has been applied to a variety of tasks, including robot manipulation [36, 47, 50], autonomous driving [12, 23, 30, 44, 59], game playing [4, 35, 51], and piloting an aircraft [21, 49]. These works have shown that IL is a training method that deserves further research.

As the IL approach learns action policies directly from expert demonstrations, *i.e.*, neither relying on rule-based predefined policies nor cumbersome manual data annota-

¹Computer Vision Center (CVC) and ²Dpt. Ciències de la Computació, Universitat Autònoma de Barcelona (UAB), Spain

Corresponding author: diego.porres@cvc.uab.es

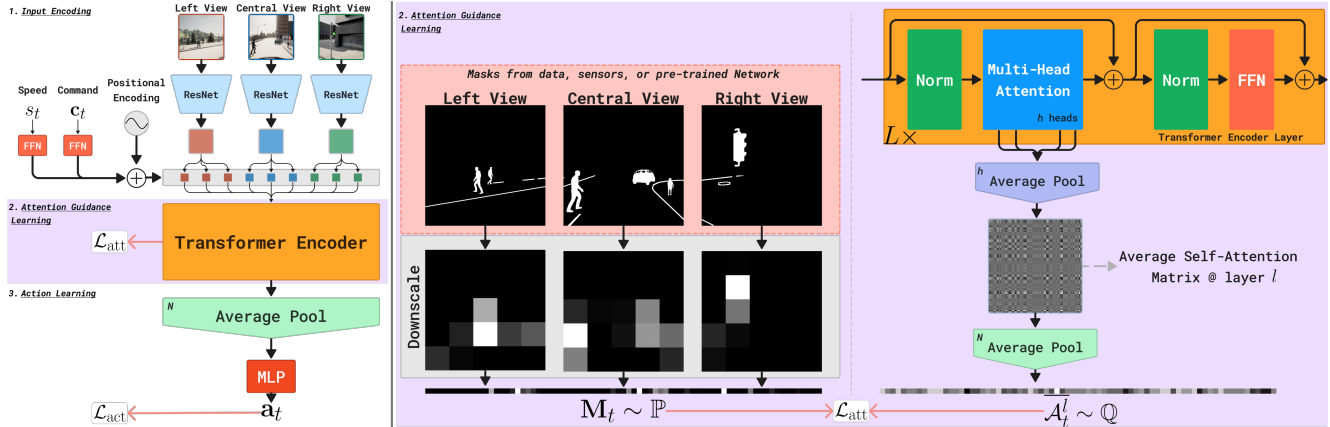


Figure 1. Our proposed pipeline. Left: the CIL++ [59] architecture. Right: our proposed Attention Loss \mathcal{L}_{att} obtained from masks using pre-computed data, on-board sensors, or a pre-trained network. For additional details, refer to Section 3.2 and 3.3, respectively.

tion, it has been a compelling research topic in autonomous driving [12, 13, 30, 34, 37, 44, 52, 58, 59, 62]. These pioneering works illustrate the possibility of mapping sensor data straight to the vehicle’s control signals (steering angle and brake/throttle) through the use of deep neural networks, without the need for intermediate modules such as semantic perception and local path planning.

As with any data-driven method, IL needs to address the dataset bias problem and causal confusion [7, 13]. Moreover, understanding the causality between the input and the output is difficult since no explicit intermediate semantic representation is available.

2.2. Attention Guidance Learning

The human visual system makes use of attention mechanisms to facilitate efficient processing. Indeed, human eyes capture redundant visual inputs that the brain can naturally process to highlight only relevant information for the targeted goal. This encourages including similar mechanisms to develop deep learning models. For instance, this idea has already brought benefits in many Computer Vision tasks [5, 8, 19, 22, 25, 31, 40, 48, 55, 56]. Including attention in Computer Vision can be traced back to 2014, when Mnih *et al.* [43] presented an RNN model that is capable of extracting information from an image or video by an adaptive selection of a sequence of regions that are then only processed at high resolution. Jaderberg *et al.* [33] introduced a learnable module, the Spatial Transformer, that allows networks to not only select regions of an image that are most relevant but also to transform them into a canonical simplified representation. More recently, along with the proposals of Transformer models such as BERT [16] and ViT [19], the idea of self-attention [53] has rapidly attracted great interest. Various Transformer-based variants such as XLNet [61], PCT [24], Swin-Transformer [39], and Transfuser [10]

have shown that attention-based models have the potential to be a powerful and general architecture in Computer Vision.

Broadly speaking, these attention mechanisms are generic and learn the specificity of the model tasks by training with enough, diverse, and representative data, which is not always available. Therefore, for vision-based driving-related tasks, different works have been proposed to explicitly force attention on specific image regions instead of learning them from scratch. The idea is to predict a saliency map that is used as an additional input channel to the RGB ones [6, 17] or is used to weight the RGB channels [20]. Sometimes these saliency maps are computed as a prediction of where human drivers would be gazing at [57]. A different approach is to use such saliency maps not as an input to the model under training but to add a loss factor to guide attention [14]. This last approach is conceptually aligned and potentially complementary to others that use some auxiliary perceptual tasks (*e.g.*, depth estimation [32], semantic segmentation [9, 30, 32, 54], object detection [54]), aiming at improving driving performance in end-to-end driving models.

2.3. Our Method in Context

In this paper, we are interested in pure vision-based end-to-end driving models trained by imitation learning. These can lead to very affordable solutions for autonomous driving as there is no need for extra sensors or costly data annotation; however, they still require more research for reliability and explainability. For this reason, we will focus on the current state-of-the-art pure vision-based end-to-end driving model CIL++ [59], but we believe that the proposed method can be applied even to non-pure-vision models in the future. All of our experiments will run on the CARLA simulator [18].

We assess how to force attention at training time through

pre-computed saliency maps, which we hypothesize can turn into better driving performance. In contrast to [6, 17, 42], we neither force additional input channels nor perform mask-based input-image weighting, which allows us to avoid predicting these masks during driving. Unlike Cultrera *et al.* [14], we exploit the self-attention maps in the architecture to highlight regions of interest without a need to *select* regions in the image and discard the rest.

The proposed saliency maps consist of binary masks highlighting task-specific classes of interest: vehicles, pedestrians, traffic signs, lane marks, and road borders. However, as these saliency maps are available at training time, and we want to keep a setting where no manual labeling of images is performed, in practice we can assume that such masks can be provided by synth-to-real unsupervised domain adaptation (StR UDA) models [26, 29]. Nonetheless, we can assume these predicted masks to be noisy, and we will show our method is robust enough even with noisy masks.

Furthermore, in our experience, providing visual activation maps to help interpret CIL++ actions has been unsuccessful. In other words, even if the model drives perfectly, the obtained activation maps are far from human-readable. Applying our method to guide attention can produce intuitive activation maps, thus, opening the door for reintroducing interpretability in end-to-end driving models.

3. Attention Learning for End-to-End Driving

3.1. Problem Setup

Our model is trained via IL, where an expert driver provides a set of driving demonstrations that can be imitated by an agent in an end-to-end manner. Following an optimal driving policy π^* that maps each instance of observations to the available action space, the expert driver performs actions \mathbf{a}_i based on a set of observations \mathbf{o}_i of the current environment, *i.e.*, $\pi^*(\mathbf{o}_i) = \mathbf{a}_i$. Thus, to effectively train an agent, we use the expert driver to collect a dataset comprised of observation/action pairs $\mathcal{D} = \{(\mathbf{o}_i, \mathbf{a}_i)\}_{i=1}^T$. The agent will follow a policy π_θ that approximates the expert policy π^* via the general imitation learning objective

$$\pi_\theta = \arg \min_{\theta} \mathbb{E}_{(\mathbf{o}_i, \mathbf{a}_i) \sim \mathcal{D}} [\mathcal{L}(\pi_\theta(\mathbf{o}_i), \mathbf{a}_i)] . \quad (1)$$

At testing time, only the trained policy $\pi_\theta(\mathbf{o}_i)$ will be used to drive the agent.

3.2. Architecture

Fig. 1 illustrates the overall architecture of our proposed model. Broadly, we can lump our model in the following three phases: Input Encoding, Attention Guidance Learning, and Action Learning.

3.2.1 Input Encoding

We keep the same setting as in CIL++ [59]. Concretely, at each timestep t the input to the network consists of three parts: 1) a set of K RGB images of dimensions $W \times H$ from the K cameras $\mathbf{X}_t = \{\mathbf{x}_{1,t}, \dots, \mathbf{x}_{K,t}\}$, 2) the forward speed of the ego vehicle $s_t \in \mathbb{R}$, and 3) a high-level (one-hot) navigation command \mathbf{c}_t that indicates which of the M commands the ego vehicle should follow.

We encode each of the K RGB images via a shared-weight ResNet backbone pre-trained on ImageNet [15, 27]. The embedded output for each view is a set of feature maps from the last convolutional layer of ResNet, thus with a shape of $w \times h \times c$ (c indicating the feature dimension). We flatten these feature maps along the spatial dimensions and concatenate them, resulting in $N = K \cdot w \cdot h$ tokens of dimension c . In addition, we linearly project the forward ego vehicle speed and the high-level navigation command to this same dimension c via separate fully connected layers, and add them to the token sequence. To provide the positional information for each token, we add a learnable positional embedding to the entire sequence. In practice, we use $K = 3$ RGB cameras (left, central, and right cameras) each with dimensions $W = H = 300$ pixels, and set $c = 512$ to match the dimensionality of the last ResNet block.

3.2.2 Attention Guidance Learning

CIL++ [59] adopts the self-attention mechanism of a Transformer Encoder block to associate relevant information across the $K = 3$ views. We keep the same setting, leveraging the self-attention layers to associate features across views. As shown in Fig. 1, our Transformer Encoder block consists of $L = 4$ multi-head attention layers. Each one includes a Multi-headed Self-Attention (MHSA) [53] block with $h = 4$ heads, layer normalization (LN) [1], and feed-forward MLP blocks (FFN). The hidden dimension D of the Transformer Encoder is set equal to the ResNet output dimension, *i.e.*, $D = c = 512$. Unlike the vanilla CIL++ training scheme, we select one of these L layers to apply the Attention Loss to, which we further expand in Section 3.3.2.

3.2.3 Action Learning

The output of the Transformer Encoder is the same shape as the input sequence, namely $N \times c$. We apply a global average pooling (GAP) along the sequence dimension N , obtaining a vector of dimension $1 \times c$. This vector is fed into an MLP consisting of two fully connected layers with ReLU non-linearity. The final output action $\hat{\mathbf{a}}_t = (\hat{a}_{s,t}, \hat{a}_{acc,t})$ comprises of the steering angle and acceleration, the latter being the difference between throttle and brake [59, 62]. We

normalize both actions to lie in the range of $[-1, 1]$, where negative values correspond to turning left or braking, and positive values correspond to turning right or accelerating, respectively for $\hat{a}_{s,t}$ and $\hat{a}_{acc,t}$.

3.3. Loss Function

The total loss function is weighted by two parts: the *Action Loss* and the *Attention Loss*:

$$\mathcal{L} = \lambda_{act}\mathcal{L}_{act} + \lambda_{att}\mathcal{L}_{att} \quad (2)$$

where $\lambda_{act}, \lambda_{att} \in \mathbb{R}^+$ indicate the weight given to the Action and Attention Loss, respectively, which we explain in the following two phases.

3.3.1 Action Loss

At each timestep t , given a predicted action $\hat{\mathbf{a}}_t \in \mathbb{R}^2$ by our network and a ground truth action $\mathbf{a}_t \in \mathbb{R}^2$ by the expert driver, we define the *Action Loss* as:

$$\mathcal{L}_{act}(\mathbf{a}_t, \hat{\mathbf{a}}_t) = \lambda_s \|\hat{a}_{s,t} - a_{s,t}\|_1 + \lambda_{acc} \|\hat{a}_{acc,t} - a_{acc,t}\|_1, \quad (3)$$

where $\|\cdot\|_1$ is the L_1 distance and $\lambda_s, \lambda_{acc} \in \mathbb{R}^+$ indicate the weights given to the steering angle and acceleration parts, respectively.

3.3.2 Attention Loss

We add an attention-learning branch to prompt an end-to-end driving model to intentionally heed safety-critical regions in the input images. At each timestep t and for each camera i , these regions will be defined via a single-channel synthetic attention mask $\mathcal{M}_{i,t} \in \mathbb{R}^{W \times H}$.

To render these attention masks used as ground truth, we make assumptions about the focus of a regular driver while driving. Specifically, we make use of the semantic segmentation and depth images provided by the CARLA simulator. These features enable us to precisely isolate and emphasize specific objects or areas within the visual field of the driving simulation. Our attention masks highlight safety-critical dynamic objects such as cars and pedestrians, and static objects that are essential for navigation and driving decisions such as traffic lights, road signs, lane markings, and road borders. These are crucial indicators of the physical space within which the car can maneuver. Furthermore, we incorporate a depth threshold in our attention mask algorithm to ensure that the driver’s attention is realistically focused on elements within a practical and safe range of the ego vehicle.

We hypothesize that the attention maps of the Transformer Encoder can effectively approximate the distribution of the attention masks. To achieve this, we first down-scale the K masks to $w \times h$, matching the spatial resolution in the Input Encoding phase. We flatten, concatenate

them, then normalize this sequence, resulting in a mask $\mathbf{M}_t \in \mathbb{R}^N$ that follows the target distribution, *i.e.*, $\mathbf{M}_t \sim \mathbb{P}$. We take advantage of the distributional property of the self-attention maps of the Transformer Encoder and force them to match \mathbb{P} . In practice, we select a layer l , get the average attention matrix of the h heads, average it row-wise $\overline{\mathcal{A}}_t^l = \mathbb{E}_N[\mathbb{E}_h[\mathcal{A}_t^{h,l}]] \in \mathbb{R}^N$, and then compare both distributions using the Kullback-Leibler (KL) divergence as our *Attention Loss*. We can reformulate it pointwise (and time-step-wise) as:

$$\mathcal{L}_{att}(\mathbf{M}_t, \overline{\mathcal{A}}_t^l) = \sum_{j=1}^N \mathbf{M}_t^j \log \left(\epsilon + \frac{\mathbf{M}_t^j}{\overline{\mathcal{A}}_t^j + \epsilon} \right) \quad (4)$$

where ϵ is a small number added for regularization. In practice, we apply this loss at the last layer $l = L = 4$, but there is no limitation on which layer to apply it to, nor to which heads. We leave the latter for future work.

Realistic Masks We define a function $f(\mathcal{M}_{i,t})$ to introduce realistic noise into masks $\mathcal{M}_{i,t}$ using depth-aware Perlin noise [45], creating variable intensity ‘blobs’ that mimic real-world imperfections. It is refined so that the distortions extend beyond simple blobs, introducing more granular disturbances on larger objects like cars and red lights. It deliberately excludes thinner features such as lane markings, which are too subtle for detailed granularity. This enhancement more accurately simulates typical real-world noise artifacts that arise from sensor or cumulative errors by StR UDA models [26, 29]. Fig. 2 showcases examples of our noise-integrated masks.

4. Experiments

4.1. Driving Environments

We conduct our experiments on the CARLA simulator [18], version 0.9.13. Regarding the expert driver used for data collection, we use a *teacher* model (agent) from [62] which is based on reinforcement learning and thus shows a more realistic and diverse behavior than the default expert driver in CARLA. We keep the same settings of CIL++ [59], using three forward-facing onboard cameras that cover a horizontal field-of-view of 180° in total (60° for each camera without overlapping). For the input RGB images, the resolution is set to $W \times H = 300 \times 300$ pixels.

To ensure consistency and reliability in our assessment, we used the same agent for all the training datasets. Data collection occurred at a rate of 10 FPS, given a spectrum of weather conditions and towns within the CARLA environment. The resulting datasets, namely the 14 and 55-hour datasets, were generated to validate and show the efficacy of our approach under varying weather conditions.

The **14-hour dataset**, acquired in `Town01`, featured eight hours of driving with a "busy" object density as specified in [62]. This dataset further diversified its scenarios by allocating two hours to each of the `ClearNoon`, `ClearSunset`, `HardRainNoon`, and `WetNoon` weather conditions. An additional six hours were recorded under the same weather conditions but with an empty object map. As `Town01` is built with single-lane roads, there are $M = 4$ vehicle commands in this dataset: *turning left*, *turning right*, *continue straight*, and *follow the lane*.

In contrast, the **55-hour dataset** was designed to explore the adaptability of our approach in a more complex environment, spanning `Town01` to `Town06`. This dataset contains diverse driving scenarios, including multi-lane driving, highways, and crossroads. Consequently, the command set for this dataset expands to $M = 6$, incorporating the commands defined in the 14-hour dataset and introducing lane-change directives: *change to left lane* and *change to right lane*.

4.2. Validation

We will validate the trained models in an online manner (using dynamic agents), so we will not use a static dataset. This evaluation is done by driving in specific scenarios and evaluating the driving quality of the agent. During this, we set the CARLA simulator in a *synchronous* manner, that is, the model can be validated without being affected by its inference time.

When training with the 14-hour dataset and its smaller subsets, we validate in the unseen `Town02` from CARLA as it also contains single-lane roads. We use the `NoCrash` setup [13] with two different weather conditions than those seen during training. For the 55-hour dataset, we use the offline Leaderboard from CARLA, using 10 distinct routes in `Town05` under two new validation weather configurations. In both, the new weather configurations are `SoftRainSunset` and `WetSunset`.

In the `NoCrash` setup, the ego agent continues to navigate until reaching the end of the route, unless it collides with some object or a time-out happens, irrespective of other driving infractions. This is not the case for the offline Leaderboard where crashes may occur. For both, we report the following key metrics extracted from the CARLA Leaderboard benchmark:

- **Success Rate (SR)** indicates the percentage of routes where the car successfully reaches the destination. It serves as a measure of the agent’s ability to complete the designated routes.
- **Route Completion (RC)** is the average of the route the ego vehicle managed to accomplish (as a percent) for all routes.
- **Infraction Score (IS)** is a scoring metric that quantifies the number of driving infractions on each route, which

include collisions with objects, ignoring traffic lights and stop signals and other rule violations. "No infractions" is indicated as 1, decreasing with every infraction.

- **Driving Score (DS)** is the product of the RC and IS per route. This is a combined metric that considers all aspects of a driving agent.

We repeat our driving test three times with different random seeds, as we randomly spawn and control the other vehicles and pedestrians in the simulator. This way, we aim to offer a detailed and quantitative assessment of our agent’s performance in diverse driving scenarios.

4.3. Training Hyperparameters

In our experiments, the CIL++[59] public code serves as the framework for executing our trials. Regardless of the dataset employed for training, we adopt the hyperparameter settings outlined in [59] to ensure consistency in our model training. Throughout all experiments, we keep the Action Loss weights the same, *i.e.*, $\lambda_{act} = 1$ and $\lambda_s = \lambda_{acc} = 0.5$. The training process spans 80 epochs with a batch size of 512 and initial learning rate of 10^{-4} , and the best-performing model, determined during training, is selected for evaluation.

To optimize the performance of our models, we systematically explore different values for the Attention Loss weight, using a small dataset comprising all the collected "busy" data in `Town01` (consisting of 8 hours of driving): $\lambda_{att} \in \{0.1, 0.25, 0.5, 1.0, 2.5, 5.0, 10.0\}$. We validate these models in `Town01` under different weather conditions to those seen during training. Our experiments show that a higher weight in Attention Loss significantly enhances results, showing a notable improvement of up to 47 points in the Success Rate metric compared to cases where attention loss is not applied. Based on these findings, we adopt a value of $\lambda_{att} = 10$.

4.4. Quantitative Results

In our experimental design, we categorize the results into two distinct sections: the *low data regime* and the *high data regime*. The low data regime is specifically dedicated to evaluating the performance of our approach when confronted with a lack of data along two axes: low availability (number of driving hours) and low variability (decreasing the types of weather conditions in the dataset).

On the other hand, the high data regime is strategically designed to compare results with robust datasets and various baselines relevant to our work. This division of our experimental results facilitates an analysis of the adaptability, robustness, and comparative performance of our approach across different data availability scenarios.

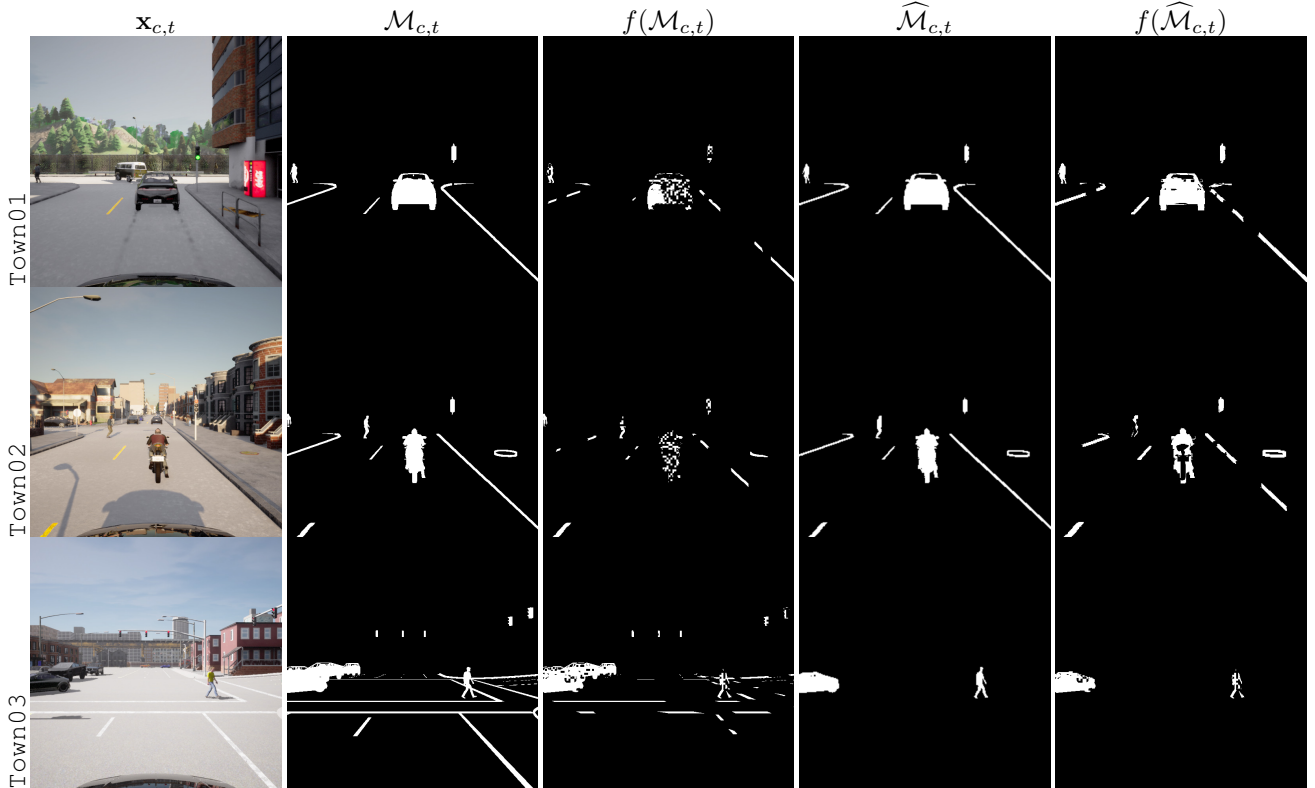


Figure 2. $\mathbf{x}_{c,t}$ (central RGB images at a timestep t) and their corresponding masks $\mathcal{M}_{c,t}$ for Town01, Town02, and Town03. For the single-lane (top rows), we use a maximum depth of 20 meters to generate the masks, whereas we use a maximum depth of 40 meters for the multi-lane towns. Note that the U²-NET was trained only with data from Town01, so the failure to detect the lanes on Town03 is merely illustrative.

4.4.1 Low data regime

To assess the impact of training with Attention Loss, we conduct experiments using incremental subsets of the 14-hour dataset with a relatively busy traffic density, randomly sampled starting from 2 hours and increasing in 2-hour increments up to 8 hours. Additionally, we include results obtained with the full 14-hour dataset for a comprehensive comparison.

The results, presented in Fig. 3, highlight the performance improvement when employing Attention Loss. When examining the baseline results for the 2-hour and 4-hour subsets, it becomes evident that the limited data availability hinders the driver’s performance, reflected in a lower SR metric of only 0 and 16 points respectively, half the performance with more extensive datasets. Conversely, when Attention Loss is applied, the dependency on large amounts of data diminishes. Even with only 4 hours of data, the model achieves a notable average SR metric of 65, representing a significant improvement of 49 points compared to the case when the model is trained without Attention Loss. Furthermore, when we add data using Attention Loss, the IS metric shows a clear improvement in driving quality.

While our proposed approach demonstrates superior performance in scenarios with limited data, concerns about potential generalization issues arise with a lack of diverse cases. To address this, we conduct experiments by sampling the 8-hour dataset based on the accumulation of different weather conditions to evaluate behavior against a change in domain. Note that combining all 4 kinds of weather results in the same 8-hour dataset registered in Fig. 3. Fig. 4 reveals that the baseline struggles to generalize effectively even when all 4 kinds of weather are included. Although it obtains a high IS score when using one weather, this is due to the agent not moving, which can be appreciated in a low RC score. In contrast, our approach demonstrates consistent gains in all metrics as we add new weather types to the training dataset, obtaining similar results with only 2 weathers compared to the 4 weathers used in the vanilla model.

These observations emphasize the robustness of using the proposed Attention Loss when confronted with challenges such as insufficient or low-variation data. This resilience contributes to the effectiveness of our approach in scenarios with limited training samples and potential domain shifts.

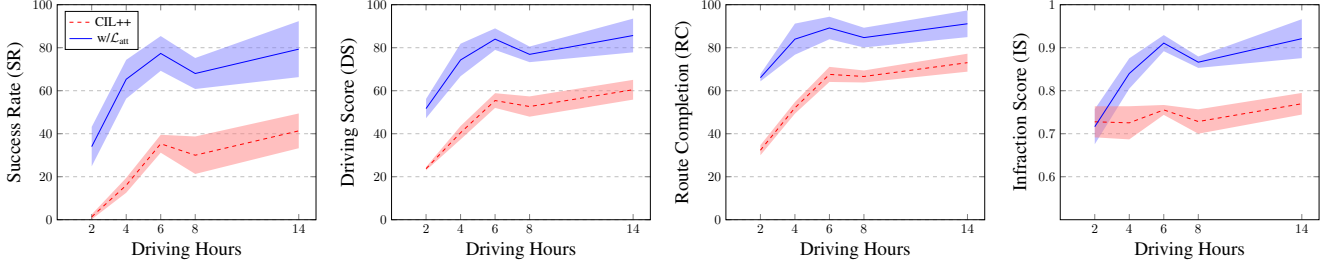


Figure 3. Comparison between the baseline (CIL++ default training) and our method (with \mathcal{L}_{att}) while increasing the amount of training data.

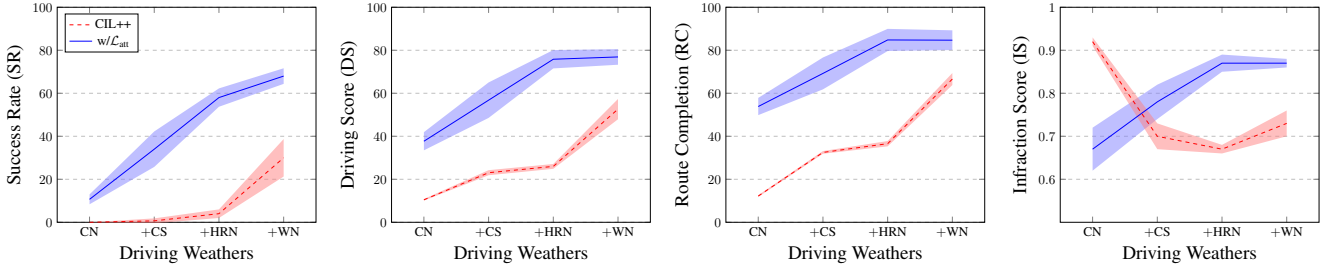


Figure 4. Driving results by incrementally adding a weather condition to the training set (2 hours of data per weather).

4.4.2 High data regime

In the context of incorporating attention maps during training, two common approaches are employed: Soft Mask (SM) and Hard Mask (HM). The SM method involves adding the attention map as a fourth channel concatenated to the camera images that we pass as input to the driving model. Conversely, the HM method utilizes an element-wise product between the attention mask and the camera image, emphasizing regions indicated by the mask. Unlike our method, both of these methods require attention maps during the inference phase. To this end, we employed the U²-NET model [46], trained on the 14-hour dataset. Qualitative results showing predicted masks $\widehat{\mathcal{M}}$ from the U²-NET on training data (Town01) and unseen data (Town02 and Town03) are depicted in Fig. 2, illustrating the similarity between the predicted and ground truth masks.

Table 1 presents results from different approaches incorporating attention masks using the 14-hour dataset. The first observation is that the inclusion of attention masks consistently improves results over the baseline, except for the SM method, which gets similar driving performance. The comparison between our approach and the HM method shows a 13% increase in completed routes, along with a longer average driving time and fewer infractions for our approach. Following the results with noisy masks we can see the same conclusions although the performance is lower for all attention-based methods due to the included noise. Note that both SM and HM methods need to have the attention mask during testing, which we avoid by only needing

Table 1. Masks as different types of input and effect of noisy masks (train: 14h Data Town01, test: Town02, New weathers)

	SR \uparrow	DS \uparrow	RC \uparrow	IS \uparrow
CIL++	41.33 \pm 8.08	60.45 \pm 4.60	73.03 \pm 4.18	0.77 \pm 0.03
w/SM	42.00 \pm 7.21	59.29 \pm 5.49	70.12 \pm 4.32	0.78 \pm 0.02
w/HM	66.00 \pm 9.17	77.34 \pm 6.93	84.32 \pm 5.83	0.87 \pm 0.04
w/ \mathcal{L}_{att}	79.33 \pm 13.01	85.67 \pm 7.84	91.13 \pm 6.21	0.92 \pm 0.05
w/SM + $f(\widehat{\mathcal{M}}_{i,t})$ ^a	35.33 \pm 7.02	56.38 \pm 1.32	68.38 \pm 0.58	0.77 \pm 0.01
w/HM + $f(\widehat{\mathcal{M}}_{i,t})$	66.00 \pm 7.21	76.36 \pm 3.72	83.46 \pm 4.48	0.87 \pm 0.01
w/ \mathcal{L}_{att} + $f(\mathcal{M}_{i,t})$ ^b	71.33 \pm 6.11	80.36 \pm 6.88	89.46 \pm 3.97	0.87 \pm 0.05

^a $f(\widehat{\mathcal{M}}_{i,t})$: Noisy predicted Masks ^b $f(\mathcal{M}_{i,t})$: Noisy Masks

it during training.

To expand our experiments to scenarios with abundant data and more complex cases, we used the 55-hour dataset. This dataset introduces challenges such as multi-lanes, highways, and crossroads. Examining the results in Table 2, the gap between the baseline and our approach is reduced here, yet our approach still outperforms, completing 3% more routes with increased average distance coverage. However, the biggest difference lies in the quality of the agent driving, where our approach achieves a higher average IS, improving from 0.5 to 0.7. These results demonstrate the effectiveness of our training method when using large datasets to enhance driving quality without the need for additional perception modules during the driving phase.

Table 2. Effect of using the attention loss in the high data regime (train: 55h Data, test: Town05, New weathers)

	SR \uparrow	DS \uparrow	RC \uparrow	IS \uparrow
CIL++	70.00 \pm 5.00	36.46 \pm 4.03	79.69 \pm 3.84	0.51 \pm 0.04
w/ \mathcal{L}_{att}	73.33 \pm 5.77	58.23 \pm 4.71	82.88 \pm 1.28	0.70 \pm 0.03

4.5. Qualitative Results

Visualizations of the resulting attention maps for the Transformer Encoder can be found in Fig. 5. For the scenario in Town01, even though both models correctly predict to break for the incoming pedestrian, CIL++’s attention maps lack *explainability*. Differently, thanks to the Attention Loss during training, our method provides quite *explainable* and *interpretable* visualizations of the attention on the sensory input. We can observe that the model has learned to segment the objects belonging to the classes of interest without needing an additional network to perform this task or to remove part of its input via masking, even in the much harder scenario in Town03. As a potential approach to reveal deep neural models’s black-box characteristics, we encourage this work to be further explored by the community to better learn the correlation between input data and output values, beyond end-to-end driving models.

5. Conclusions

In this paper, we demonstrate how it is possible to guide the attention of a pure-vision end-to-end driving model by introducing a (noisy) saliency semantic map loss, without model architecture modification. Thus, no increasing computational resources are required at testing time. Using CIL++ as a reference model and the CARLA simulator with its standard benchmarks, we provide rich experimental results to show that our method is superior to others that require the computation of saliency maps at testing time. Our method also helps to obtain more intuitive activation maps, which we plan to use as behavior explanations in natural language. In the same vein, we plan to leverage this research to explore the field of causal correlation learning for deep learning models. Lastly, encouraged by the results using noisy attention masks, we plan to test the Attention Loss with real data and deploy the model in a real car.

Acknowledgements

This research is supported by project TED2021-132802B-I00 funded by MCIN/AEI/10.13039/501100011033 and the European Union NextGenerationEU/PRTR. Antonio M. López acknowledges the financial support to his general research activities given by ICREA under the ICREA Academia Program. Antonio and Gabriel thank the synergies, in terms of research ideas, arising from the project PID2020-115734RB-

C21 funded by MCIN/AEI/10.13039/501100011033. The authors acknowledge the support of the Generalitat de Catalunya CERCA Program and its ACCIO agency to CVC’s general activities.

References

- [1] Jimmy Lei Ba, Jamie Ryan Kiros, and Geoffrey E Hinton. Layer normalization. arXiv:1607.06450, 2016. 3
- [2] Dzmitry Bahdanau, Kyunghyun Cho, and Yoshua Bengio. Neural machine translation by jointly learning to align and translate. arXiv:1409.0473, 2014. 1
- [3] Stephen Lehmkuhle Barbara A. Steinman, Scott B. Steinman. Visual attention mechanisms show a center-surround organization. In *Vision Research*, pages 1859–1869, 1995. 1
- [4] Jeffrey Barratt and Chuanbo Pan. Deep imitation learning for playing real time strategy games. *Cs229 Stanf. Edu*, 2019. 1
- [5] Irwan Bello, Barret Zoph, Ashish Vaswani, Jonathon Shlens, and Quoc V Le. Attention augmented convolutional networks. In *International Conference on Computer Vision (ICCV)*, 2019. 1, 2
- [6] Xuelai Du Ce Zhang, Azim Eskandarian. Attention-based neural network for driving environment complexity perception. In *Intelligent Transportation Systems Conference (ITSC)*, 2021. 2, 3
- [7] Li Chen, Penghao Wu, Kashyap Chitta, Bernhard Jaeger, Andreas Geiger, and Hongyang Li. End-to-end autonomous driving: Challenges and frontiers. *arXiv preprint arXiv:2306.16927*, 2023. 2
- [8] Tseng-Hung Chen, Yuan-Hong Liao, Ching-Yao Chuang, Wan-Ting Hsu, Jianlong Fu, and Min Sun. Show, adapt and tell: Adversarial training of cross-domain image captioner. In *International Conference on Computer Vision (ICCV)*, 2017. 1, 2
- [9] Kashyap Chitta, Aditya Prakash, and Andreas Geiger. NEAT: Neural attention fields for end-to-end autonomous driving. In *International Conference on Computer Vision (ICCV)*, 2021. 2
- [10] Kashyap Chitta, Aditya Prakash, Bernhard Jaeger, Zehao Yu, Katrin Renz, and Andreas Geiger. Transfuser: Imitation with transformer-based sensor fusion for autonomous driving. *IEEE Trans. on Pattern Analysis and Machine Intelligence*, 2022. 2
- [11] Kyunghyun Cho, Bart Van Merriënboer, Caglar Gulcehre, Dzmitry Bahdanau, Fethi Bougares, Holger Schwenk, and Yoshua Bengio. Learning phrase representations using rnn encoder-decoder for statistical machine translation. arXiv:1406.1078, 2014. 1
- [12] Felipe Codevilla, Matthias Müller, Antonio M. López, Vladlen Koltun, and Alexey Dosovitskiy. End-to-end driving via conditional imitation learning. In *International Conference on Robotics and Automation (ICRA)*, 2018. 1, 2
- [13] Felipe Codevilla, Edgar Santana, Antonio M. López, and Adrien Gaidon. Exploring the limitations of behavior cloning for autonomous driving. In *International Conference on Computer Vision (ICCV)*, 2019. 2, 5

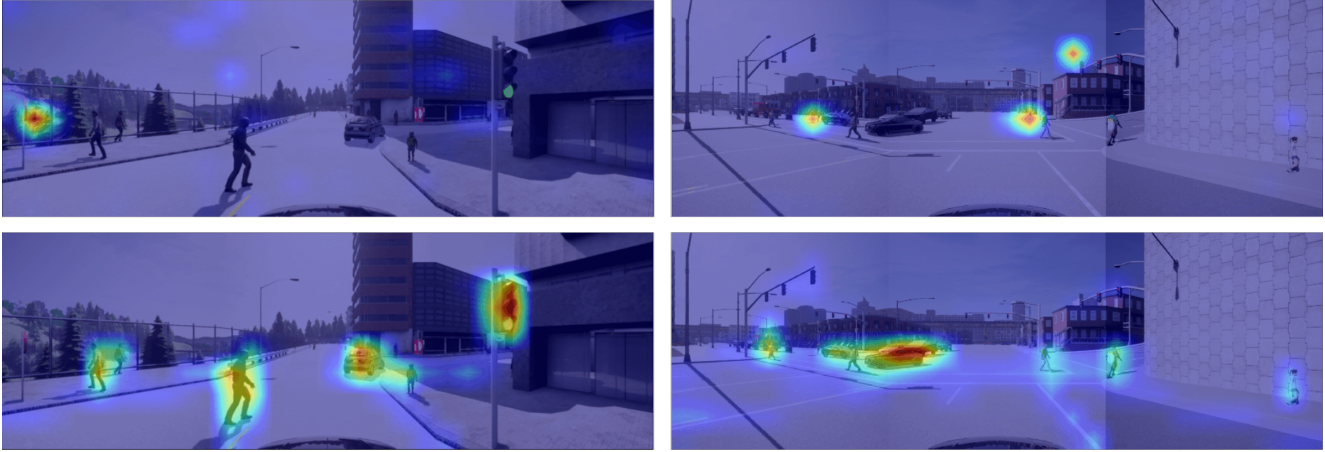


Figure 5. Visualization of the average attention map of the last layer of the Transformer Encoder using three RGB cameras as input for CIL++ (top row) and CIL++ with the Attention Loss \mathcal{L}_{att} (bottom row), for Town01 (left column) and Town03 (right column).

- [14] Luca Cultrera, Federico Becattini, Lorenzo Seidenari, Pietro Pala, and Alberto Del Bimbo. Explaining autonomous driving with visual attention and end-to-end trainable region proposals. *Journal of Ambient Intelligence Humanized Computing*, 2023. 2, 3
- [15] Jia Deng, Wei Dong, Richard Socher, Li-Jia Li, Kai Li, and Li Fei-Fei. ImageNet: A large-scale hierarchical image database. In *International Conference on Computer Vision and Pattern Recognition (CVPR)*, 2009. 3
- [16] Jacob Devlin, Ming-Wei Chang, Kenton Lee, and Kristina Toutanova. Bert: Pre-training of deep bidirectional transformers for language understanding, 2018. 1, 2
- [17] Ning Ding, Ce Zhang, and Azim Eskandarian. Saliendet: A saliency-based feature enhancement algorithm for object detection for autonomous driving. *IEEE Trans. on Intelligent Vehicles*, 2023. 2, 3
- [18] Alexey Dosovitskiy, German Ros, Felipe Codevilla, Antonio López, and Vladlen Koltun. CARLA: An open urban driving simulator. In *Conference on Robot Learning (CoRL)*, 2017. 1, 2, 4
- [19] Alexey Dosovitskiy, Lucas Beyer, Alexander Kolesnikov, Dirk Weissenborn, Xiaohua Zhai, Thomas Unterthiner, Mostafa Dehghani, Matthias Minderer, Georg Heigold, Sylvain Gelly, Jakob Uszkoreit, and Neil Houlsby. An image is worth 16x16 words: Transformers for image recognition at scale. In *International Conference on Learning Representation (ICLR)*, 2021. 2
- [20] Aldo Aldo Faisal. Predicting visual attention of human drivers boosts the training speed and performance of autonomous vehicles. *Journal of Vision*, 21:2819, 2021. 2
- [21] Henrique Freitas, Rui Camacho, and Daniel Castro Silva. Performing aerobatic maneuver with imitation learning. In *International Conference on Computational Science*, 2023. 1
- [22] Jun Fu, Jing Liu, Haijie Tian, Yong Li, Yongjun Bao, Zhiwei Fang, and Hanqing Lu. Dual attention network for scene segmentation. In *International Conference on Computer Vision and Pattern Recognition (CVPR)*, 2019. 1, 2
- [23] Laurent George, Thibault Buhet, Emilie Wirbel, Gaetan LeGall, and Xavier Perrotton. Imitation learning for end to end vehicle longitudinal control with forward camera. In *Neural Information Processing Systems (NIPS) Imitation Learning WS*, 2018. 1
- [24] Meng-Hao Guo, Jun-Xiong Cai, Zheng-Ning Liu, Tai-Jiang Mu, Ralph R Martin, and Shi-Min Hu. Pct: Point cloud transformer. *Computational Visual Media*, 7:187–199, 2021. 2
- [25] Meng-Hao Guo, Tian-Xing Xu, Jiang-Jiang Liu, Zheng-Ning Liu, Peng-Tao Jiang, Tai-Jiang Mu, Song-Hai Zhang, Ralph R Martin, Ming-Ming Cheng, and Shi-Min Hu. Attention mechanisms in computer vision: A survey. *Computational visual media*, 8(3):331–368, 2022. 2
- [26] Jose L. Gómez, Gabriel Villalonga, and Antonio M. López. Co-training for unsupervised domain adaptation of semantic segmentation models. *Sensors*, 23:621, 2023. 3, 4
- [27] Kaiming He, X. Zhang, Shaoqing Ren, and Jian Sun. Deep residual learning for image recognition. *2016 IEEE Conference on Computer Vision and Pattern Recognition (CVPR)*, pages 770–778, 2015. 3
- [28] Sepp Hochreiter and Jürgen Schmidhuber. Long short-term memory. *Neural computation*, 9(8):1735–1780, 1997. 1
- [29] Lukas Hoyer, Dengxin Dai, Haoran Wang, and Luc Van Gool. MIC: Masked image consistency for context-enhanced domain adaptation. In *International Conference on Computer Vision and Pattern Recognition (CVPR)*, 2023. 3, 4
- [30] Anthony Hu, Gianluca Corrado, Nicolas Griffiths, Zak Murez, Corina Gurau, Hudson Yeo, Alex Kendall, Roberto Cipolla, and Jamie Shotton. Model-based imitation learning for urban driving. In *Neural Information Processing Systems (NeurIPS)*, 2022. 1, 2
- [31] Jie Hu, Li Shen, and Gang Sun. Squeeze-and-excitation networks. In *International Conference on Computer Vision and Pattern Recognition (CVPR)*, 2018. 1, 2
- [32] Keishi Ishihara, Anssi Kanervisto, Jun Miura, and Ville Hautamäki. Multi-task learning with attention for end-to-end

- autonomous driving. In *International Conference on Computer Vision and Pattern Recognition (CVPR) Workshop on Autonomous Driving*, 2021. 2
- [33] Max Jaderberg, Karen Simonyan, Andrew Zisserman, et al. Spatial transformer networks. *Advances in neural information processing systems*, 28, 2015. 2
- [34] Arez Jamgochian, Etienne Buehrle, Johannes Fischer, and Mykel J Kochenderfer. Shail: Safety-aware hierarchical adversarial imitation learning for autonomous driving in urban environments. In *International Conference on Robotics and Automation (ICRA)*, 2023. 2
- [35] Emilio Jorge, Mikael Kågeback, Fredrik D Johansson, and Emil Gustavsson. Learning to play guess who? and inventing a grounded language as a consequence. arXiv:1611.03218, 2016. 1
- [36] Heecheol Kim, Yoshiyuki Ohmura, Akihiko Nagakubo, and Yasuo Kuniyoshi. Training robots without robots: deep imitation learning for master-to-robot policy transfer. *IEEE Robotics and Automation Letters*, 8(5):2906–2913, 2023. 1
- [37] Xiaodan Liang, Tairui Wang, Luona Yang, and Eric Xing. CIRL: Controllable imitative reinforcement learning for vision-based self-driving. In *European Conf. on Computer Vision (ECCV)*, 2018. 2
- [38] Grace W. Lindsay. Attention in psychology, neuroscience, and machine learning. *Frontiers in Computational Neuroscience*, 14, 2020. 1
- [39] Ze Liu, Yutong Lin, Yue Cao, Han Hu, Yixuan Wei, Zheng Zhang, Stephen Lin, and Baining Guo. Swin transformer: Hierarchical vision transformer using shifted windows. In *International Conference on Computer Vision (ICCV)*, 2021. 2
- [40] Jiasen Lu, Caiming Xiong, Devi Parikh, and Richard Socher. Knowing when to look: Adaptive attention via a visual sentinel for image captioning. In *International Conference on Computer Vision and Pattern Recognition (CVPR)*, 2017. 1, 2
- [41] Minh-Thang Luong, Hieu Pham, and Christopher D Manning. Effective approaches to attention-based neural machine translation. arXiv:1508.04025, 2015. 1
- [42] Alexander Makrigiorgos, Ali Shafti, Alex Harston, Julien Gerard, and A Aldo Faisal. Human visual attention prediction boosts learning & performance of autonomous driving agents. *arXiv preprint arXiv:1909.05003*, 2019. 3
- [43] Volodymyr Mnih, Nicolas Heess, Alex Graves, et al. Recurrent models of visual attention. *Advances in neural information processing systems*, 27, 2014. 2
- [44] Yunpeng Pan, Ching-An Cheng, Kamil Saigol, Keuntaek Lee, Xinyan Yan, Evangelos A Theodorou, and Byron Boots. Agile autonomous driving using end-to-end deep imitation learning. In *Robotics: Science and Systems (RSS)*, 2018. 1, 2
- [45] Ken Perlin. Improving noise. In *Proceedings of the 29th annual conference on Computer graphics and interactive techniques*, 2002. 4
- [46] Xuebin Qin, Zichen Zhang, Chenyang Huang, Masood Dehghan, Osmar Zaiane, and Martin Jagersand. U2-net: Going deeper with nested u-structure for salient object detection. page 107404, 2020. 7
- [47] Nathan D. Ratliff, James A. Bagnell, and Siddhartha S. Srinivasa. Imitation learning for locomotion and manipulation. In *International Conference on Humanoid Robots (HUMANOIDS)*, 2007. 1
- [48] Steven J Rennie, Etienne Marcheret, Youssef Mroueh, Jerret Ross, and Vaibhava Goel. Self-critical sequence training for image captioning. In *International Conference on Computer Vision and Pattern Recognition (CVPR)*, 2017. 1, 2
- [49] Claude Sammut, Scott Hurst, Dana Kedzier, and Donald Michie. Learning to fly. In *Machine Learning Proceedings 1992*, pages 385–393. 1992. 1
- [50] Simon Stepputtis, Joseph Campbell, Mariano Phielipp, Stefan Lee, Chitta Baral, and Heni Ben Amor. Advances in neural information processing systems. In *Neural Information Processing Systems (NIPS)*, 2020. 1
- [51] Chaitanya Thammineni, Hemanth Manjunatha, and Ehsan T Esfahani. Selective eye-gaze augmentation to enhance imitation learning in atari games. *Neural Computing and Applications*, 35(32):23401–23410, 2023. 1
- [52] Learning to drive from simulation without real world labels. Bewley, alex and rigley, jessica and liu, yuxuan and hawke, jeffrey and shen, richard and lam, vinh-dieu and kendall, alex. In *International Conference on Robotics and Automation (ICRA)*, 2019. 2
- [53] Ashish Vaswani, Noam Shazeer, Niki Parmar, Jakob Uszkoreit, Llion Jones, Aidan N Gomez, Łukasz Kaiser, and Illia Polosukhin. Attention is all you need. In *Neural Information Processing Systems (NeurIPS)*, 2017. 1, 2, 3
- [54] Dan Wang, Junjie Wen, Yuyong Wang, Xiangdong Huang, and Feng Pei. End-to-end self-driving using deep neural networks with multi-auxiliary tasks. *Automotive Innovation*, 2, 2019. 2
- [55] Fei Wang, Mengqing Jiang, Chen Qian, Shuo Yang, Cheng Li, Honggang Zhang, Xiaogang Wang, and Xiaoou Tang. Residual attention network for image classification. In *International Conference on Computer Vision and Pattern Recognition (CVPR)*, 2017. 1, 2
- [56] Sanghyun Woo, Jongchan Park, Joon-Young Lee, and In So Kweon. Cbam: Convolutional block attention module. In *European Conf. on Computer Vision (ECCV)*, pages 3–19, 2018. 1, 2
- [57] Ye Xia, Jinkyu Kim, John Canny, Karl Zipser, and David Whitney. Periphery-fovea multi-resolution driving model guided by human attention. In *Winter conf. on Applications of Computer Vision (WACV)*, 2020. 2
- [58] Yi Xiao, Felipe Codevilla, Akhil Gurram, Onay Urfalioglu, and Antonio M López. Multimodal end-to-end autonomous driving. *IEEE Trans. on Intelligent Transportation Systems*, 23(1):537–547, 2020. 2
- [59] Yi Xiao, Felipe Codevilla, Diego Porres, and Antonio M López. Scaling vision-based end-to-end autonomous driving with multi-view attention learning. In *International Conference on Intelligent Robots and Systems (IROS)*, 2023. 1, 2, 3, 4, 5
- [60] Zichao Yang, Diyi Yang, Chris Dyer, Xiaodong He, Alex Smola, and Eduard Hovy. Hierarchical attention networks for document classification. In *Proceedings of the 2016 conference of the North American chapter of the association*

for computational linguistics: human language technologies, 2016. [1](#)

- [61] Zhilin Yang, Zihang Dai, Yiming Yang, Jaime Carbonell, Russ R Salakhutdinov, and Quoc V Le. Xlnet: Generalized autoregressive pretraining for language understanding. *Advances in neural information processing systems*, 32, 2019. [1](#), [2](#)
- [62] Zhejun Zhang, Alexander Liniger, Dengxin Dai, Fisher Yu, and Luc Van Gool. End-to-end urban driving by imitating a reinforcement learning coach. In *International Conference on Computer Vision (ICCV)*, 2021. [2](#), [3](#), [4](#), [5](#)